Environ. Sci. Technol. **2010,** *44,* 6319–6324

Evaluating Adsorption and Biodegradation Mechanisms during the Removal of Microcystin-RR by Periphyton

YONGHONG WU,*,†,§ JIANGZHOU HE,‡ AND LINZHANG YANG*,†

State Key Laboratory of Soil and Sustainable Agriculture, Institute of Soil Science, Chinese Academy of Sciences No. 71, East Beijing Road, Nanjing 210008, P. R. China, College of Life Science, Tarim University, Shihezi Alar 843300, P. R. China, and Graduate University of Chinese Academy of Sciences, Beijing 100049, P. R. China

Received July 15, 2009. Revised manuscript received June 17, 2010. Accepted July 6, 2010.

Microcystin-RR (MCRR) is among the cyanobacterial toxins of significant concern due to their negative effects on water quality and human health. In this study, periphyton dominated by bacteria and diatoms was applied to remove MCRR from water. The maximum removal rate of MCRR by periphyton was observed in the first day (the latent adaptation period). Within this period, 85.2%, 73.3%, 83.5%, and 86.5% of the total MCRR removed (through adsorption and biodegradation) was by the adsorption of periphyton when the periphyton biomasses were 1.32 g, 3.96 g, 6.60 g, and 9.24 g, respectively. The amount of MCRR adsorbed increased with the increasing ratio of periphyton biomass to MCRR in solution. The adsorption process fitted well to the Freundlich, Langmuir, and Dubinin−Radushkevich (D-R) models, implying that the bioadsorption process has mechanistic relevance. The MCRR adsorption by periphyton is physical in nature and thermodynamically spontaneous. This study provided strong evidence that adsorption was the main mechanism for the removal of MCRR and other microcystins by periphyton and similar microbial aggregates in the latent adaptation period. Thereafter, biodegradation of periphyton dominated the toxin removal process. These results show that periphyton can be employed for an environmentally benign and effective solution for MCRR removal.

Introduction

Among the cyanotoxins often produced when toxic cyanobacterial blooms occur, microcystins produced by *Microcystis aeruginosa* are commonly detected in water bodies (*1*). These microcystins can cause adverse effects on both animal and human health (*2*). There are more than 60 types of microcystins identified to date, of which MCRR is the most common species found worldwide (*3*).

Many methods have been applied to remove cyanobacteria and their microcystins (*4*). Among these methods, the technique of using microorganisms (and/or biofilms) capable of degrading microcystins is widely accepted. Methods employing microcystin-degrading microorganisms can be classified into two groups. One is entirely ascribed to biofilms grown on the surface of substrates within bioreactors such as biological sand (*5, 6*), granular activated carbon filters (*7*), biofilm-reactors based on immobilized microorganisms (*8*), and biological treatment facilities combined with conventional treatment processes (*9*). The other group depends on specific microorganisms that possess effective microcystin-degrading activities, such as bacteria (*Sphingpoyxis* sp.) (*10*) and (*Sphingomonas* sp.) (*11, 12*).

These methods however, may not be highly effective when applied to the treatment of surface waters due to a number of limitations. First, using bioreactors such as sand filters require drawing the surface water samples through bioreactors. This process involves high operation costs thereby making the method impractical for large-scale treatment of surface waters. In addition, bioreactors based on biofilms generally require a maturation phase, the time taken for a microorganism population to establish. This maturation phase may take weeks or even months (*13, 14*). Similarly, the methods employing specific microcystin-degrading microorganisms may require an acclimation period prior to microcystin degradation, during which the microorganisms isolated from surface waters are incubated under appropriate conditions. The longer the acclimation phase the greater the risk of exposure of animals and humans to these toxins (*6*). Moreover, some microcystin-degrading microorganisms are unable to entirely adapt to the actual conditions of the surface waters and eventually die.

Periphyton is essentially a type of biofilm in surface waters, composed of attached floral and faunal microorganisms that grow on submerged surfaces (*15*). In freshwater, periphyton biofilms are more commonly found than other biofilms (*15, 16*). They are native to the surface waters of freshwater, so they will require shorter maturation and acclimation times in such water matrices. Furthermore, the production site of microcystins is generally in surface waters during harmful cyanobacterial blooms. Thus, using periphyton originating from surface waters to remove microcystins has practical significance. A similar material, phototrophic biofilm from river ecosystems, has successfully been used to remove microcystins (*17*). However, the composition of this biofilm was relatively simple, mostly dominated by phototrophic microorganisms such as coccal green alga *Oocystis lacustirs* or composed of colonial green alga *Protoderma* sp. and diatoms *Navicula* sp. and *Achnanthes* sp (*17*). Such simple biofilm composition may be susceptible to variable surface water conditions making it difficult to form a stable and self-recycling microecosystem in surface water. Therefore, in our experiments, we examined the microcystin removal effectiveness of a more complex biofilm: periphyton, composed of heterotrophic and phototrophic microorganisms.

Microcystins can be removed by biodegradation and/or adsorption activities of the microorganisms (or microbial aggregates). To date most attention has focused on the biodegradation of microcystins by microorganisms. For example, some microorganisms isolated from microbial aggregates such as bacteria with mlrA gene (*5*) from sand filters and microorganisms in sediment (*18*) can remove microcystins solely by biodegradation (*5, 6, 10, 11*). It is well-known that the structure of periphyton (biofilm) ranges from patchy monolayers to filamentous accretions during different phases of biofilm formation (*19*). The basic structure of biofilm aggregations include at least three conceptual models:

* Corresponding author phone (fax): +86-25-86881591; e-mail: yhwu@issas.ac.cn (Y.W.), lzyang@issas.ac.cn (L.Y.).
† Chinese Academy of Sciences No. 71.
§ Graduate University of Chinese Academy of Sciences.
‡ Tarim University.

10.1021/es903761y
Published on Web 07/16/2010

(i) heterogeneous mosaic biofilm aggregations, (ii) penetrated water-channel biofilms, and (iii) dense confluent biofilms (*20*). Due to the special porous structure of periphyton biofilms, the dynamics of pollutants adsorbed to or desorbed from the active sites on the periphyton surface can occur concomitantly, such as that of nutrients freely transporting into periphytons (*21*). Therefore, we propose that the removal of MCRR by periphyton depends on the mechanisms of both adsorption and biodegradation.

The primary objectives of this study were to determine whether MCRR can be effectively removed by periphyton biofilm and to provide clearer insight into the individual adsorption and biodegradation MCRR removal mechanisms by discriminating between MCRR removal achieved by each process. A third objective was to explain the adsorption process of MCRR using isotherm models (Langmuir, Freundlich, Dubinin−Radushkevich) and adsorption behavior using mathematical models (adsorption intensity, sorption energy, and Gibbs free energy). The findings will (i) provide a promising environmentally benign biomeasure to remove MCRR in surface waters that suffered from harmful cyanobacterial blooms and (ii) assist in improving the MRCC removal efficiency by periphyton and similar microbial aggregates by distinguishing (or modulating) adsorption and biodegradation mechanisms in different growth phases of microbial aggregates.

Materials and Methods

Periphyton Culture. Glass slides (25.4 × 76.2 mm) sterilized by 0.1 M HCl solution for 3 × 30 min were submerged and fixed in a nutrient-enriched water filtrate (through 0.45 μm pore) obtained from a hypereutrophic lake and used to culture the periphyton. The periphyton cultures were incubated at 25−30 °C with aeration (dissolved oxygen level was kept at 7.0−9.5 mg L^{-1}) until dense periphyton was formed after 36 days. The dense periphyton biofilms with their substrates (glass slides) were then used in the following trials.

MCRR Removal Experiment. Four different treatment levels were tested in this experiment, each with different number of periphyton slides. Either 1, 3, 5, or 7 slides with the pregrown periphyton were placed into a 6.0-L glass tank containing 5.0-L of sterilized nutrient-enriched water filtrate (through 0.22 μm pore). For the control, sterilized slides (using 0.1 M HCl solution for 3 × 30 min) were rinsed with aseptic fresh double-distilled water three times. Seven of these slides were put into the sterilized nutrient-enriched water filtrate (through 0.22 μm pore) in each tank. MCRR (purity >85%, from Institute of Hydrobiology, Chinese Academy of Sciences) was directly added into each tank to an initial MCRR concentration of 500 μg L^{-1}. Over the course of the experiment, the tanks were kept indoors away from the light to avoid MCRR photodegradation. The temperature was kept constant at 25 °C. The amount of MCRR removed was calculated by subtracting the remnant MCRR concentration in the solution from the initial MCRR concentration. This experiment was repeated three times for each treatment level.

MCRR Adsorption Experiment. Triplicate batch adsorption experiments were carried out by adding 1, 3, 5, or 7 slides with pregrown periphyton into 6.0-L glass tanks containing 5.0 L of filtered nutrient-enriched (through 0.22 μm pore) water of pH 7.5. The corresponding weights of adsorbent (the total weight of periphyton biomass at 25−30 °C, moisture 85 ± 1%) were 1.32 g, 3.96 g, 6.60 g, and 9.24 g, respectively. Thereafter, 5.0 g of sodium azide (NaN_3) was added to each tank to inhibit microbial activity. For the control, sterilized slides (using 0.1 M HCl solution for 3 × 30 min) were rinsed with aseptic fresh double-distilled water three times. Seven of these slides and 5.0 g of NaN_3 were added to the sterilized nutrient-enriched water filtrate (through 0.22 μm pore) in each tank. MCRR was directly added to each tank with the initial MCRR concentration in each treatment level (1.32 g, 3.96 g, 6.60 g, and 9.24 g periphyton), and the corresponding control was kept at fixed value as follows: 71.8 μg L^{-1}, 100.5 μg L^{-1}, 167.5 μg L^{-1}, and 502.5 μg L^{-1}. Each tank was wrapped in a piece of cloth so as to prevent photodegradation and placed on a shaker (150 rpm) for 24 h at 25 °C.

Adsorption Test Experiment. To distinguish the adsorption due to the biodegradation of periphyton for MCRR removal in the latent adaptation period, the following experiment was performed in triplicate. A sterilized slide with 1.0 g of periphyton (25−30 °C, moisture 85%) was placed into the 100 mL flask containing 50 mL of filtered nutrient-enriched water (through 0.22 μm pore) of pH 7.5. After the microbial activity was inhibited by the addition of NaN_3, MCRR was directly added to each flask up to an initial MCRR concentration of 500 μg L^{-1} as in the adsorption experiment. Each flask was wrapped in a piece of cloth so as to prevent photodegradation and placed on a shaker (150 rpm) for 24 h at 25 °C. The MCRR concentrations in solution and periphyton were determined at regular intervals.

Analysis and Statistics. In order to estimate biomass, the periphyton grown for 36 days was collected from 10 slides with a sterile knife. The peeled-off biomass was filtered (through 0.45 μm pore) and dried at 25−30 °C to 85 ± 1% moisture content. The average periphyton biomass of each slide was 1.32 g. The morphology of periphyton was characterized by scanning electron photomicrograph (SEM, Philips Xl30S-FEG).

Characterization of the bacteria with flaA gene in the periphyton was conducted using ERIC-PCR techniques as these bacteria are common in fresh waters (*22, 23*). The detailed operation process is presented in the Supporting Information (SI). MCRR concentrations in water and periphyton were determined according to widely used methods with the detailed operation described in the SI. Microbial respiration was measured with a respirometer as the rate of CO_2−C efflux during 40 h of incubation at 20 °C (*24*).

As each experiment was repeated three times, the mean results are presented. Statistical analysis (Paired-Samples *t* test) was performed using SPSS 12.0. A $p < 0.05$ indicated statistical significance.

For adsorption isotherms, MCRR solutions at different concentrations (71.8−502.5 μg L^{-1}) were agitated with a known amount of adsorbent for a period of 24 h. The remnant MCRR concentration (C_t) of the solution was then determined. The concentration retained in the periphyton phase (q_e and q) was calculated by the following equations

$$q_e = \frac{(C_0 - C_e)V}{W_s} \quad (1)$$

and

$$q = \frac{(C_0 - C_t)V}{W_s} \quad (2)$$

In order to determine the MCRR adsorption characteristics of periphyton and to evaluate the applicability of this adsorption process, adsorption thermodynamic experiments were carried out at 298.15 K. Models such as the Freundlich and Langmuir isotherms were applied to analyze the experimental data.

Based on further analysis of the Langmuir equation, the dimensionless parameter of the equilibrium or adsorption intensity (R_L) can be expressed by

$$R_L = \frac{1}{1 + K_L C_0} \quad (3)$$

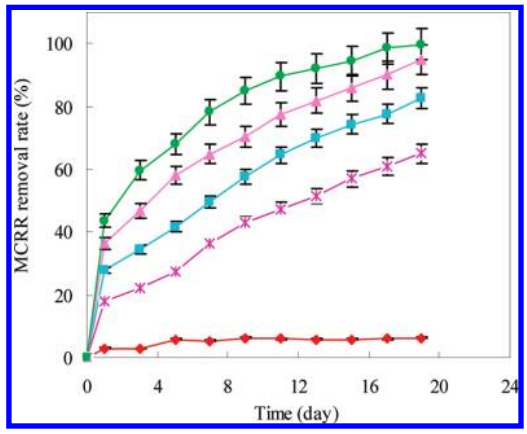

FIGURE 1. Removal rates of MCRR by different biomasses of periphyton through adsorption and biodegradation processes (without added NaN_3). The initial MCRR concentration was 500 μg L^{-1}.

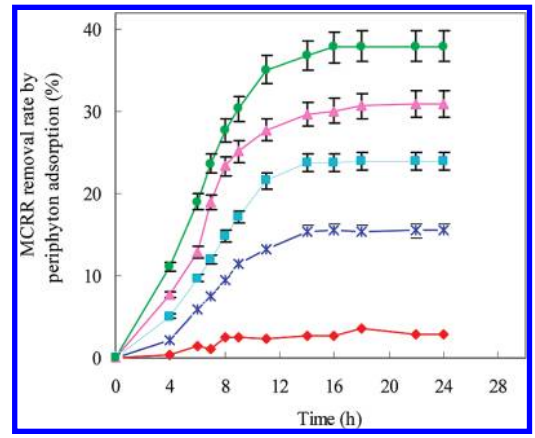

FIGURE 2. MCRR removal rates by different biomasses of periphyton through adsorption (with added NaN_3). The initial MCRR concentration was 500 μg L^{-1}.

The R_L parameter is considered to be one of the more reliable indicators of the adsorption intensity of a surface. There are four possibilities for the R_L value: (1) favorable adsorption, $0 < R_L < 1$, (2) unfavorable adsorption, $R_L > 1$, (3) linear adsorption, $R_L = 1$, and (4) irreversible adsorption, $R_L = 0$ (*25, 26*).

The Dubinin−Radushkevich (D-R) isotherm model was also used to determine the adsorption type (physical or chemical). The linear form of the D-R model is expressed by

$$\ln q_e = \ln q_m - \beta\varepsilon^2 \quad (4)$$

where ε is the Polanyi potential [$\varepsilon = RT \ln (1 + (1)/(C_e))$].

Thermodynamic parameters such as sorption energy (E) and Gibbs free energy ($\Delta G°$) were evaluated in order to study the feasibility of the process and application of the present adsorbent. The mean sorption energy and Gibbs free energy were calculated based on the equilibrium constant values, β and K_L, respectively. Their equations [eq (1S) and eq (2S)] are presented in the SI.

Results and Discussion

Periphyton Characteristics. The periphyton community was composed primarily of bacteria and diatoms (SI, Figure 1S.a). Periphyton characterization showed that the diatoms included the following: *Melosira varians* Ag., *Gomphonema parvulum* Kütz., *Synedra ulna* Kütz., *Nitzschia amphibia* Grun., and *Fragilaria vaucheriae* Kütz. Most bacteria found were bacilli and cocci. The bands obtained for the test samples in the ERIC-PCR fingerprint test were located in the same position as the 2kb and 1.5kb bands in the reference samples (SI, Figure 1S.b). This result is very similar to findings by Li et al. (*27*), which suggested the bacterial abundance during cultivation and in cultivated periphyton (*27*). The average Shannon-Weaver diversity index of bacteria based on flaA gene in the periphyton was 2.37, a value greater than 1.90, which implies that the bacterial community in periphyton was highly diversified (*27, 28*).

Removal of MCRR. The amount of MCRR removed in the control ranged from 0 to 6.3% between 0 to the 19th day (Figure 1). This implies that the sterilized glass slides did not significantly affect MCRR removal. The concentrations of MCRR in solution decreased rapidly after the addition of the periphyton, and the removal rate of MCRR increased with increasing periphyton biomass. The removal rates during the 19 days were 64.9%, 82.8%, 94.8%, and 99.7% for the treatment groups with 1.32 g, 3.96 g, 6.60 g, and 9.24 g of periphyton biomass, respectively. The removal rates of MCRR in the treatment groups were significantly different from that in the control ($p < 0.05$).

The slope of the dynamic curves of MCRR removal was calculated for each treatment group in each experimental period (every day). The slopes obtained for the period from the start of the experiment to day 1 were larger than those of later days, suggesting that the removal rate was highest during the first day of treatment. The overall average removal rates of MCRR in the first day were 18.1%, 27.9%, 36.3%, and 43.5% of the initial MCRR content for the treatment groups with 1.32 g, 3.96 g, 6.60 g, and 9.24 g of periphyton biomass, respectively. Individually these accounted for 27.9%, 33.7%, 38.3%, and 43.6% of the total MCRR removal amount, respectively.

Adsorption of MCRR. It has been reported that NaN_3 can suppress microbial respiration and inhibit the process of biodegradation (*29*). After the addition of NaN_3 for 1 day, the levels of microbial respiration of the periphyton in the treatment groups and microbial respiration in the water in the control were found to be zero. This suggested that the addition of NaN_3 significantly inhibited microbial activities and also implied that the effects of microorganisms on MCRR removal were not significant. The amount of MCRR removed in the control ranged from 0 to 2.9% between 0 to 24 h (Figure 2). This further suggested that the degradation of MCRR could be ignored during the adsorption experimental period.

The average MCRR removal rates by adsorption within 24 h were 15.5%, 23.4%, 30.3%, and 37.6% for the treatment groups with 1.32 g, 3.96 g, 6.60 g, and 9.24 g of periphyton biomass, respectively. These accounted for 85.2%, 73.3%, 83.5%, and 86.5% of the total amount of MCRR being removed (through adsorption and biodegradation) on the first day (Figure 2). This indicated that the MCRR adsorption by periphyton dominated the MCRR removal on the first day, while many previous studies have paid little attention to this adsorption process (*5, 6, 10, 11*). The average MCRR adsorption rates by periphyton biomasses rapidly increased with time up to 14 h. Thereafter, the amount of MCRR adsorbed to periphyton remained almost constant from the 16−24th hours in all the treatment groups (Figure 2). This implied that the amount of MCRR adsorbed into periphyton was close to saturation. From this period onward, the MCRR removal by periphyton was largely dependent on biodegradation.

Figure 2 also demonstrates the influence of the adsorbent dose (periphyton biomass) on MCRR adsorption. The adsorption rate of MCRR increased with increasing periphyton dose (adsorbent dosage). This is due to a larger surface area available for adsorption and more cavities on the adsorbent allowing easier penetration of the MCRR molecule to the sorption sites (*19*−*21*). The MCRR adsorption

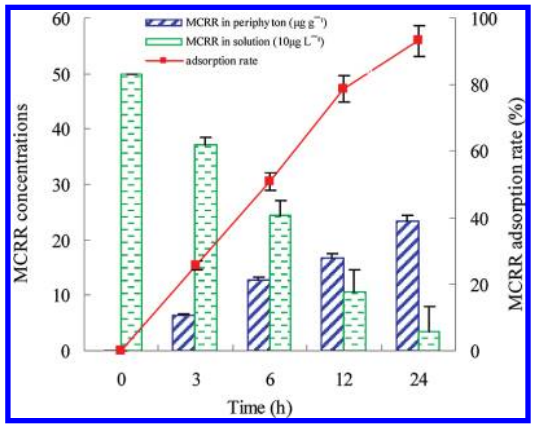

FIGURE 3. Concentration of MCRR adsorbed into periphyton and that remaining in solution and the corresponding MCRR removal rates by periphyton adsorption (with added NaN_3). The initial ratio of periphyton biomass to MCRR amount in solution was 4×10^4.

rate increased with an increase in the initial periphyton biomass to MCRR amount in solution ratio (from 0.5×10^3 to 3.7×10^3). This implies that the periphyton might have mechanistic relevance like physical solid sorbents such as peat (*30*) and activated carbon (*31, 32*).

Balance of MCRR in Periphyton and Solution. To verify the adsorption process, the balance of MCRR in periphyton in the absence of biodegradation was calculated by determining the MCRR concentrations in periphyton and solution. The MCRR concentration in solution decreased over time from 500 to 34.1 μg L^{-1} between 0 and 24 h, while the average MCRR concentration in the periphyton markedly increased from 0 to 23.3 μg g^{-1} between 0 and 24 h (Figure 3). This indicates that the MCRR in the periphyton had been adsorbed from aqueous solution. Based on the changes in adsorption rate, it was found that the MCRR removal rate by periphyton adsorption increased rapidly from 0 to 78.7% between 0 to 12 h, thereafter the MCRR absorption rate started to decrease, resulting in 78.7% to 93.2% of MCRR being removed between 12 to 24 h. This change of adsorption rate supported the results from the adsorption experiment (Figure 2). Therefore, it is confirmed that dramatic MCRR adsorption activity by periphyton occurred within the beginning and middle of the adsorption period. This is very similar to most surface adsorption processes based on physical solid sorbents such as activated carbon (*31, 32*), implying that the bioadsorption process of periphyton can be described by mechanistic models such as surface models.

The amount of MCRR removed increased with the increase of the ratio of periphyton biomass to MCRR amount in solution (Figures 2 and 3). In addition, the MCRR removal by periphyton could be entirely attributed to adsorption as soon as the initial ratio of periphyton biomass to MCRR amount in solution reached a sufficiently high value. When the initial ratio of periphyton biomass to MCRR amount in solution was 4.0×10^4, the average MCRR removal rate by periphyton adsorption in the first 24 h was 93.2%. This was higher than the highest removal rate (37.6%) in the adsorption experiment with the 9.24 g periphyton treatment. This was attributed to the ratio of periphyton biomass to MCRR amount in solution in the adsorption test experiment being higher 10 times than that of the latter. This further implied that the bioadsorption of periphyton to MCRR is mechanistically relevant.

Adsorption Isotherms. In order to optimize the design of an adsorption system to remove MCRR using periphyton in the latent adaptation period, it is important to establish the most appropriate correlation for the equilibrium curve. We believe the most important step is to understand the properties of the bioadsorption process, distinguishing which isotherms (mechanistic or empirical) are suitable for this bioadsorption process. Langmuir and Freundlich and D-R equations, as surface models, are often used to examine adsorption data collected from heterogeneous surfaces (*33*−*35*). Considering the heterogeneous surface of periphyton, Freundlich, Langmuir, and D-R isotherms were selected for this study.

TABLE 1. q_m and K_L of the Langmuir Equation and the K_F and n of the Freundlich Equation

	Langmuir equation			Freundlich equation		
treatment groups (periphyton)	K_L	q_m	R^2	log K_F	$1/n$	R^2
1.32 g	12.46	0.32	0.84	0.88	0.2599	0.85
3.96 g	25.85	0.32	0.99	0.64	0.3459	0.85
6.60 g	38.45	0.29	0.97	0.70	0.4259	0.88
9.24 g	37.96	0.20	0.97	0.95	0.4780	0.93

The equilibrium data were fitted to the linear Freundlich equation for the adsorption of MCRR onto periphyton. A satisfactory empirical isotherm can be used for nonideal adsorption because of the high coefficients of determination (R^2) obtained (Table 1). The Freundlich constant (n) ranged from 2.1 to 3.9, indicating that the adsorption of MCRR onto periphyton was favorable under the study conditions. It has been shown that n values between 1 and 10 represent good adsorption potential of the adsorbent (*31*).

The equilibrium data obtained for the adsorption of MCRR onto periphyton were fitted to the linear Langmuir equation. The linear plots of C_e/q_e versus C_e were examined to determine the q_m and K_L values. The values are given in Table 1. The high coefficients of determination (R^2) of the plots showed that the linear Langmuir equation was a good model that fit the adsorption isotherm of MCRR under the given conditions.

The variation of the adsorption intensity (R_L) with the initial concentration of the solution (C_0, mg L^{-1}) is shown in Figure 4. The R_L values ranged from 0.15 to 0.31 between 71.8 μg L^{-1} to 502.5 μg L^{-1} of initial MCRR concentrations and decreased with the increase of initial MCRR concentration. This parameter ($0 < R_L < 1$) indicated that the periphyton was an effective adsorbent for the adsorption of MCRR from an aqueous solution.

The adsorption data were also applied to the D-R isotherm model based on the heterogeneous surface of the adsorbent in order to distinguish physical adsorption from chemical adsorption. The equilibrium data were fitted to the linear D-R equation [eq 4] for the adsorption of MCRR onto periphyton at 25 °C. The β value and the monolayer sorption capacity (q_m) were calculated from the slopes and y-axis

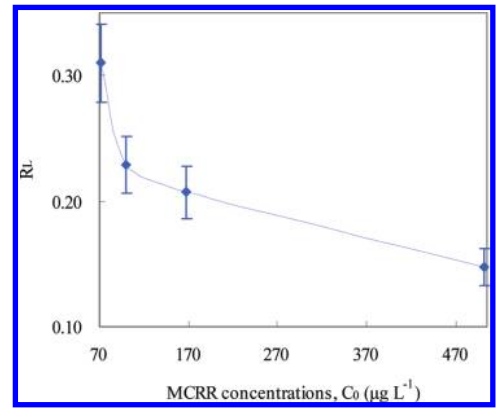

FIGURE 4. Variation in adsorption intensity with different initial MCRR concentrations.

intercepts of the plots, respectively. The β values ranged from 3×10^{-8} to 8×10^{-6} mol^2 (kJ)$^{-2}$ between 1.32 and 9.24 g of periphyton biomass.

In many cases, Freundlich, Langmuir, and D-R equations have been regarded as empirical, rather than mechanistic (e.g., surface models) adsorption isotherms models (*32, 34*). In fact, the Freundlich and D-R isotherms can have mechanistic relevance only in the unique case where sorbents have exponential distribution of adsorption energies (*36, 37*). In this study data collected from the bioadsorption process simultaneously fitted these empirical equations. This suggests that the bioadsorption of periphyton was associated with the energy distribution in periphyton. This in turn supports the use of these empirical equations in characterizing a bioadsorption process using microbial aggregates such as periphyton. This also implies that the bioadsorption process of periphyton has mechanistic relevance (or surface adsorption property) and that the model parameters included in these empirical equations have specific thermodynamic significance.

The mean sorption energy (E) can be used to distinguish chemical and physical adsorption. If the E value is between 8 and 16 kJ mol^{-1}, the adsorption process follows chemical ion-exchange (*30*). If E is less than 8 kJ mol^{-1}, then the adsorption is physical in nature (*30*). From eq (1S), the E values were between 2.50 and 4.08 kJ mol^{-1} in the different treatments with periphyton biomasses from 1.32 to 9.24 g, indicating the adsorption process is basically physical in nature.

The thermodynamic results based on eq (2S) showed that ΔG° were from -9.0 kJ mol^{-1} to -6.2 kJ mol^{-1} in the different treatments with periphyton biomasses from 1.32 to 9.24 g. As all values were less than zero, this indicated that the MCRR adsorption on periphyton was a spontaneous process.

This study demonstrated the effectiveness of MCRR removal by periphyton in surface waters using the dual removal mechanisms of adsorption and biodegradation. This is the first study to demonstrate that the rapid removal of MCRR by periphyton in the latent adaptation period was largely due to adsorption, after which time biodegradation played the key role. Adsorption of MCRR in the latent adaptation period was modeled using Freundlich, Langmuir, and Dubinin−Radushkevich (D-R) models to provide evidence that the adsorption of MCRR by periphyton was the primary removal mechanism. By applying models, it has been demonstrated that the adsorption of MCRR by periphyton in the latent adaptation period has mechanistic relevance and was a physical and spontaneous process. These results suggest that when using surface waters as the drinking water source, adding an adsorption tank based on periphyton to remove microcystins prior to the centralized drinking water treatment process can help decrease the microcystins levels. Similarly, with regards to the treatment of surface wastewaters, inclusion of the periphyton-based microcystin adsorption tank before the traditional wastewater treatment process (i.e., activated sludge method) could also improve the microcystins removal efficiency. Furthermore, outcomes from this study will assist in the development of mathematical models to simulate the adsorption mechanism for removal of MCRR and other microcystins by periphyton and similar microbial aggregates.

Acknowledgments

We sincerely appreciate Dr. Shanqing Zhang, Dr. Clare Morrison, and Dr. Trang Nguyen from Griffith University, Gold Coast, Australia, for their revision of this manuscript. This work was supported by the National Natural Science Foundation of China, the Innovative Project of Chinese Academy of Sciences (KZCX1-YW-14-5), the National High-tech R&D Program of China (2007AA06Z304) and National Key Technology R&D Program (2007BAD87B12). The authors sincerely thank three anonymous reviewers for their constructive advice.

Appendix A

q_e	mg g^{-1} the amount of MCRR adsorbed at equilibrium
q mg g^{-1}	the amount of MCRR adsorbed at a given time
C_0	mg L^{-1} the initial MCRR concentration
C_e	mg L^{-1} the MCRR concentration at equilibrium
C_t	mg L^{-1} the MCRR concentration at a given time
V	L the volume of solution
W_s	g the mass of the adsorbent
q_m	mg g^{-1} maximum possible amount of MCRR that can be adsorbed per unit dry weight of periphyton
K_L	empirical constant, indicating the affinity of adsorbent toward the adsorbate
R_L	adsorption intensity
K_F	empirical constant, indicates the adsorption capacity of the adsorbent
n	constant indicating the intensity of adsorption
β	mol^2 J^{-2} the activity coefficient related to the mean sorption energy
ε	Polanyi potential
R	J mol^{-1}K^{-1} gas constant, 8.314
T	K the absolute temperature
E	kJ mol^{-1} the mean sorption energy
ΔG°	kJ mol^{-1} Gibbs free energy

Supporting Information Available

Materials for periphyton characterization, determination method of MCRR in water, and Figure 1S. This material is available free of charge via the Internet at http://pubs.acs.org.

Literature Cited

(1) Rinta-Kanto, J. M.; Ouellette, A. J. A.; Boyer, G. L.; Twiss, M. R.; Bridgeman, T. B.; Wilhelm, S. W. Quantification of toxic *Microcystis* spp. during the 2003 and 2004 blooms in western Lake Erie using quantitative real-time PCR. *Environ. Sci. Technol.* **2005**, *39* (11), 4198–4205.

(2) Carmichael, W. W. Cyanobacteria secondary metabolites-The cyanotoxin. *J. Appl. Bacteriol.* **1992**, *72* (6), 445–459.

(3) WHO. Guidelines for Drinking-Water Quality. *Health Criteria and Other Supporting Information*, 2nd ed.;World Health Organization: Geneva, 1998.

(4) Chorus, I.; Bartram, J. *Toxic Cyanobacteria in Water: A guide to their public health consequences, monitoring and management*; E & FN Spon, WHO Press: London and New York, 1999.

(5) Ho, L.; Meyn, T.; Keegan, A.; Hoefel, D.; Brookes, J.; Saint, C. P.; Newcombe, G. Bacterial degradation of microcystin toxins within a biologically active sand filter. *Water Res.* **2006**, *40* (4), 768–774.

(6) Bourne, D. G.; Blakeley, R. L.; Riddles, P.; Jones, G. J. Biodegradation of the cyanobacterial toxin microcystin LR in natural water and biologically active slow sand filters. *Water Res.* **2006**, *40* (6), 1294–1302.

(7) Wang, H.; Ho, L.; Lewis, D.; Brookes, J. D.; Newcombe, G. Discriminating and assessing adsorption and biodegradation removal mechanisms during granular activated carbon filtration of microcystin toxins. *Water Res.* **2007**, *41* (18), 4262–4270.

(8) Tsuji, K.; Asakawa, M.; Anzai, Y.; Sumino, T.; Harada, K. Degradation of microcystins using immobilized microorganism isolated in an eutrophic lake. *Chemosphere* **2006**, *65* (1), 117–124.

(9) Saitou, T.; Sugiura, N.; Itayama, T.; Inamori, Y.; Matsumura, M. Degradation of microcystin by biofilm in practical treatment facility. *Water Sci. Technol.* **2002**, *46* (11/12), 237–244.

(10) Ho, L.; Hoefel, D.; Saint, C. P.; Newcombe, G. Isolation and identification of a novel microcystin-degrading bacterium from a biological sand filter. *Water Res.* **2007**, *41* (20), 4685–4695.

(11) Saito, T.; Okano, K.; Park, H.; Itayama, T.; Inamori, Y.; Neilan, B.; Burns, B.; Sugiura, N. Detection and sequencing of the microcystin LR-degrading gene, mlrA, from new bacteria isolated from Japanese lakes. *FEMS Microbiol. Lett.* **2003**, *229* (2), 271–276.

(12) Valeria, A.; Ricardo, E.; Stephan, P.; Alberto, W. Degradation of microcystin-RR by *Sphingomonas* sp. CBA4 isolated from San Roque reservoir (Córdoba - Argentina). *Biodegradation* **2006**, *17* (5), 447–455.
(13) Zhang, S.; Huck, P. M. Parameter estimation for biofilm processes in biological water treatment. *Water Res.* **1996**, *30* (2), 456–464.
(14) Bruce, A. M.; Hawkes, H. A. *Biological Filters*; Academic Press: London, 1983.
(15) Sladeckova, A. Limnological investigation methods for the periphyton ('Aufwuchs') community. *Bot. Rev.* **1962**, *28* (2), 286–350.
(16) Keevil, C. W.; Godfree, A.; Holt, D.; Dow, C. Allelochemical control of natural photoautotrophic biofilms. In *Biofilms in the Aquatic Environment;* Royal Society of Chemistry, Special Publication (Royal Society of Chemistry (Great Britain): Cambridge, 1999; pp 320−326.
(17) Babica, P.; Blaha, L.; Marsalek, B. Removal of microcystins by phototrophic biofilms. A microcosm study. *Environ. Sci. Pollut. Res.* **2005**, *12* (6), 369–374.
(18) Holst, T.; Jøgensen, N. O. G.; Jøgensen, C.; Johansen, A. Degradation of microcystin in sediments at oxic and anoxic, denitrifying conditions. *Water Res.* **2003**, *37* (19), 4748–4760.
(19) Wolf, G.; Picioreanu, C.; van Loosdrecht, M. C. M. Kinetic modeling of phototrophic biofilms-the PHOBIA model. *Biotechnol. Bioeng.* **2007**, *97* (5), 1064–1079.
(20) Wimpenny, J. W. T.; Colasanti, R. A unifying hypothesis for the structure of microbial biofilms based on cellular automaton models. *FEMS Microbiol. Ecol.* **1997**, *22* (1), 1–16.
(21) Scinto, L. J.; Reddy, K. R. Biotic and abiotic uptake of phosphorus by periphyton in a subtropical freshwater wetland. *Aquat Bot.* **2003**, *77* (3), 203–222.
(22) Gondo, T.; Sekizuka, T.; Manaka, N.; Murayama, O.; Millar, B. C.; Moore, J. E.; Matsuda, M. Demonstration of the shorter flagellin (flaA) gene of urease-positive thermophilicCampylobacter isolated from the natural environment in Northern Ireland. *Folia Microbiol. (Prague, Czech Repub.)* **2006**, *51* (3), 183–190.
(23) Sekizuka, T.; Murayama, O.; Moore, J. E.; Millar, B. C.; Matsuda, M. Flagellin gene structure of *flaA* and *flaB* and adjacent gene loci in urease-positive thermophilic *Campylobacter* (UPTC). *J. Basic Microb.* **2007**, *47* (1), 63–73.
(24) Nordgren, A. Apparatus for the continuous, long-term monitoring of soil respiration rate in large numbers of samples. *Soil Biol. Biochem.* **1988**, *20* (6), 955–957.
(25) Angove, M. J.; Johnson, B. B.; Wells, J. D. Adsorption of cadmium(II) on kaolinite. *Colloids Surf., A* **1997**, *126* (2/3), 137–147.
(26) Ho, Y. S.; Huang, C. T.; Huang, H. W. Equilibrium sorption isotherm for metal ions on tree fern. *Process Biochem.* **2002**, *37* (12), 1421–1430.
(27) Li, H.; Li, X.; Zhao, Y.; Huang, M.; Yu, X.; Jin, C.; Xu, Y. Analysis of structure changes of microbial community in medium biofilm by ERIC-PCR fingerprinting. *Environ. Sci.* **2006**, *27* (2), 2542–2546.
(28) Di Giovanni, G. D.; Watrud, L. S.; Seidler, R. J.; Widmer, F. Fingerprinting of mixed bacterial strains and BIOLOG gram-negative (GN) substrate communities by enterobacterial repetitive intergenic consensus sequence-PCR (ERIC-PCR). *Curr. Microbiol.* **1999**, *38* (4), 217–223.
(29) Saisho, D.; Nakazono, M.; Tsutsumi, N.; Hirai, A. ATP synthesis inhibitors as well as respiratory inhibitors increase steady-state level of alternative oxidase mRNA in Arabidopsis thaliana. *J. Plant Physiol.* **2001**, *158* (2), 241–245.
(30) Ho, Y. S.; McKay, G. Sorption of dye from aqueous solution by peat. *Chem. Eng. J.* **1998**, *70* (2), 115–124.
(31) Kadirvelu, K.; Namasivayam, C. Activated carbon from coconut coirpith as metal adsorbent: adsorption of Cd(II) from aqueous solution. *Adv. Environ. Res.* **2003**, *7* (2), 471–478.
(32) Li, L.; Quinlivan, P.; Knappe, D. R. U. Predicting adsorption isotherms for aqueous organic micropollutants from activated carbon and pollutant properties. *Environ. Sci. Technol.* **2005**, *39* (9), 3393–3400.
(33) GarciaCalzon, J. A.; Diaz-Garcia, M. E. Characterization of binding sites in molecularly imprinted polymers. *Sens. Actuators, B* **2007**, *123* (2), 1180–1196.
(34) Kinnlburgh, D. General purpose adsorption isotherms. *Environ. Sci. Technol.* **1986**, *20* (9), 895–904.
(35) Umpleby, R. J.; Baxter, S. C.; Bode, M.; Berch, J. K.; Shah, R. N.; Shimizu, K. D. Application of the Freundlich adsorption isotherm in the characterization of molecularly imprinted polymers. *Anal. Chim. Acta* **2001**, *435* (1), 35–42.
(36) Manes, M. *Encyclopedia of Environmental Analysis and Remediation*; John Wiley: New York, 1998.
(37) Nguyen, T. H.; Sabbah, I.; Ball, W. P. Response to comment on "Sorption nonlinearity for organic contaminants with diesel soot: Method development and isotherm interpretation". *Environ. Sci. Technol.* **2004**, *38* (20), 5486–6487.

ES903761Y